

**NUCLEAR
EXPERIMENTAL TECHNIQUES**

Electron/Hadron Separation in the Electromagnetic Calorimeter of the PHENIX Setup

A. V. Bazilevskii*, S. White**, E. P. Kistenev**, V. I. Kochetkov*, and V. K. Semenov*

* Institute for High-Energy Physics, Protvino, Moscow oblast, 142284 Russia

** Brookhaven National Laboratory, USA

Received July 23, 1998

Abstract—The efficiency of $e(\gamma)/\pi$ rejection in the electromagnetic calorimeter of the PHENIX setup was measured using various discrimination methods in the 0.5–4-GeV/c momentum range and for 0°–20° angles of incidence.

The electromagnetic calorimeter (EMCal) of the PHENIX setup [1] has a hodoscope structure, optimized for analyzing processes with multiple particle production in heavy-ion interactions at the RHIC collider (BNL, USA). The main calorimeter component is a tower measuring $\sim 5.5 \times 5.5$ cm across and 18 radiation lengths in depth. The tower is a sandwich of alternating 1.5-mm-thick lead and 4-mm-thick scintillator layers [2]. The towers are grouped in modules with 4 towers in each, and 36 modules are integrated in supermodules, which form six plane sectors with dimensions of 2×4 m, distributed over a cylinder surface of 5-m radius. Neutral particles are incident on the calorimeter at angles with the normal to the calorimeter surface ranging from 0° to 20°.

One of the important tasks of the electromagnetic calorimeter consists in identifying electrons and photons and measuring their characteristics.

The efficiencies of various $e(\gamma)/\pi$ separation methods are studied for particles with energies in the 0.5–4-GeV range and angles of incidence on the calorimeter ranging between 0° and 20°. The methods of discrimination between electrons and hadrons, which are used in the experiments, are based on the difference in the following characteristics of the electromagnetic and nuclear showers in the electromagnetic-calorimeter thickness: the distribution of energy deposited in the EMCal volume, the shape of the cross shower profile, and the distribution of difference in the measured and known (from measurements with track detectors) positions of incidence. The results of this work are based on the experimental data obtained while testing the supermodule of the electromagnetic calorimeter in the sessions of 1995–1996 at the AGS accelerator (BNL, USA).

E/p-METHOD

By measuring the charged-particle momentum with track detectors and using the differences in the spectra of energies deposited by electromagnetic and hadronic

showers in the calorimeter, it is possible to efficiently discriminate between electrons and hadrons.

The characteristic length, along which a hadronic shower propagates, is related to the nuclear interaction length for this material. The module of the PHENIX electromagnetic calorimeter has a thickness of ~ 0.8 of the nuclear length. In accordance with this value, $\sim 55\%$ of the hadrons interact with the calorimeter material and initiate propagation of a nuclear cascade. Accordingly, $\sim 45\%$ of hadrons lose their energy in the calorimeter mainly due to ionization, producing an ionization peak in the spectrum of energy deposited in the calorimeter. Figure 1 shows the spectra of energy deposited in the calorimeter by incident pions, protons, and electrons with 0.5-, 1-, and 2-GeV/c momenta.

At large particle momenta such that $pc/M > 2–3$ (M is the particle mass), ionization losses in the material vary slightly with particle energy (momentum) [3]. The loss is about $E_{\text{mip}} = 200$ MeV in the module of the PHENIX electromagnetic calorimeter, that is ~ 270 MeV, when the calorimeter is energy-calibrated with electrons. The difference between these two values is due to the different specific energies deposited by minimum-ionizing particles and electrons in the lead and scintillation plates. For electromagnetic showers, the energy fraction deposited in the active module layers (scintillation plates) is approximately 19%, whereas for the ionization energy loss of relativistic particles in the calorimeter module, this value is about 26%. At smaller particle momenta, such that $pc/M < 2$, the specific ionization loss in the material increases [3]. The ionization energy loss in the calorimeter is at a maximum when a particle is stopped, having passed through the whole module length, e.g., the momentum, at which the proton free path in the calorimeter material is equal to the calorimeter-module thickness, is about 1 GeV/c. This value corresponds to the 414-MeV kinetic energy value that a proton spends for ionization (if it has failed to produce a nuclear cascade), which is ~ 570 MeV for the elec-

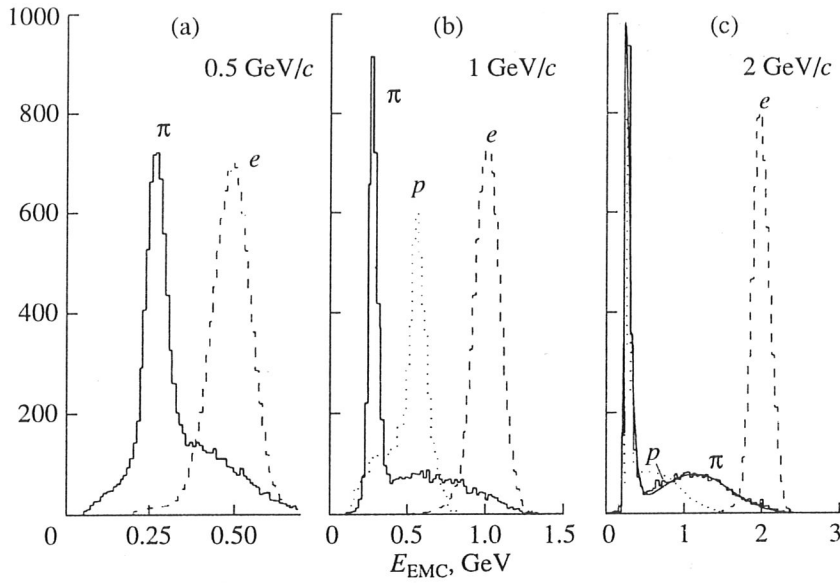


Fig. 1. The spectra of energy deposited in the calorimeter by pions, protons, and electrons with momenta of 0.5, 1, and 2 GeV/c ; the energy spectrum for pions with 2 GeV/c momentum is fitted by the sum of the Landau and Gauss distributions.

tron calibration (Fig. 1b). Pions begin stopping in the calorimeter when their momentum is about 300 MeV/c .

The spectra of energy deposited by hadrons in the electromagnetic calorimeter (see Fig. 1c) are fitted well by the sum of the Landau (ionization peak) and Gauss (for hadrons producing a cascade in the calorimeter material) distributions. The average energy deposited in the calorimeter E_{EMC} by pions that have undergone interaction (initiated the cascade) with a momentum p_π in the 0.5–4- GeV/c energy range varies linearly with the pion momenta (Fig. 2a):

$$E_{\text{EMC}}, \text{ GeV} = 0.46p_\pi + 0.23. \quad (1)$$

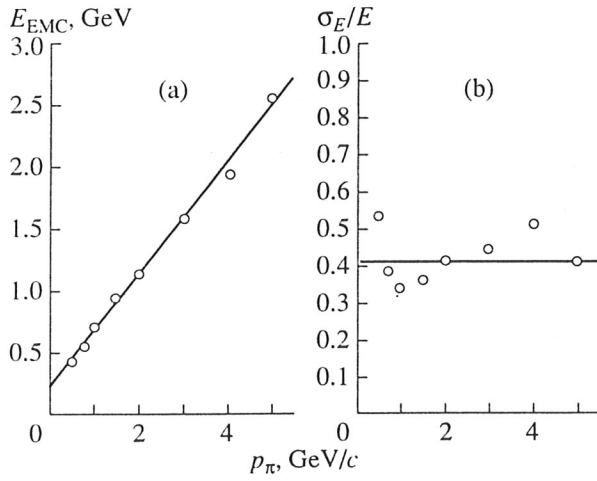


Fig. 2. (a) The average energy E_{EMC} deposited in the calorimeter and (b) the relative fluctuations of the calorimeter response for interacted pions, as a function of their momentum.

The relative fluctuations of the calorimeter response σ_E/E for interacted pions were virtually independent of the particle energy and made up ~40% (Fig. 2b). Qualitatively, the same results were obtained for the electromagnetic section of the SPACAL calorimeter [4].

The pion-detection efficiency ε_π is shown in Fig. 3a as a function of their momentum, using the criterion

$$|E_{\text{EMC}} - pc| < \alpha \sigma_E, \quad (2)$$

which corresponds to the electron-detection efficiency $\varepsilon_e = 90\%$. Here, E_{EMC} is the measured energy release in the calorimeter, p is the particle momentum, σ_E is the calorimeter energy resolution for electrons (photons), and α is the parameter determined by the value of ε_e .

METHOD BASED ON MEASURING THE CROSS SHOWER PROFILE

Use of the Shower Width

By measuring the shower widths in the electromagnetic calorimeter, it is possible to improve the e/π -separation, especially, for high energies deposited by particles in the calorimeter. The second central moment of the distribution of energy deposited by a shower in the calorimeter cells can be adopted as a shower-width measure [5–7]:

$$D_x = \frac{\sum E_i x_i^2}{\sum E_i} - \left(\frac{\sum E_i x_i}{\sum E_i} \right)^2 = \bar{x}^2 - \bar{x}^2, \quad (3)$$

where E_i is the measured energy deposited in the i th calorimeter cell, and x_i is the coordinate of its center.

The formulas for the Y -projection look like (3) (with y substituted for x). As is noted in [5, 6], the distribution of D_x depends strongly on the position of incidence on the cell. It is proposed in [6] to replace D_x with the corrected value D_x^{cor} which is virtually independent of the point of impact:

$$D_x^{\text{cor}} = D_x - D_x^{\text{min}}, \quad (4)$$

$$D_x^{\text{min}} = h\bar{x} - \bar{x}^2, \quad |\bar{x}| \leq 0.5h.$$

Here, the center of the coordinates is shifted to the center of the cell containing the center of gravity for the shower \bar{x} , and h is the dimension of the calorimeter cell. $D_x = D_x^{\text{min}}$, when the cluster has a width $n_x = 2$ cells along the X axis; for $n_x > 2$, $D_x > D_x^{\text{min}}$ [6].

The quantity similar to (3) is proposed in [8] as a shower-width measure, but with logarithms of the relative energies deposited in the detector cells used as weights:

$$D_x^{\log} = \frac{\sum w_i x_i^2}{\sum w_i} - \left(\frac{\sum w_i x_i}{\sum w_i} \right)^2, \quad (5)$$

$$w_i = \max \{0, (w_0 + \ln(E_i/E_0))\}, \quad E_0 = \sum E_i.$$

By analogy with [8], we determined the optimal value $w_0 = 4.5$, for which the best $e(\gamma)/\pi$ separation is achieved in the PbSc electromagnetic calorimeter of the PHENIX setup.

The distribution of values

$$D = D_x + D_y, \quad (6)$$

$$D^{\text{cor}} = D_x^{\text{cor}} + D_y^{\text{cor}}, \quad (7)$$

$$D^{\log} = D_x^{\log} + D_y^{\log} \quad (8)$$

for electrons and charged pions with 2-GeV energy is shown in Figs. 4a, 4b, and 4c (only the events with a deposited energy of about 2 GeV were taken into account). The cut limits corresponding to 90% detection efficiency for electromagnetic showers are marked in the figures. Figure 3b shows the detection efficiency for charged π -mesons with 4- GeV/c momenta as a function of the deposited shower energy measured in the calorimeter using cuts for D , D^{cor} , and D^{\log} , which correspond to 90% efficiency of electron (photon) detection. For energy releases in the calorimeter of more than 1 GeV, the efficiency of the $e(\gamma)/\pi$ separation is slightly higher when D^{\log} is used as a shower-width measure.

The χ^2 -Criterion

The use of the χ^2 -criterion for comparing the measured and expected cross profiles of the electromagnetic shower proves to be a more efficient method. In

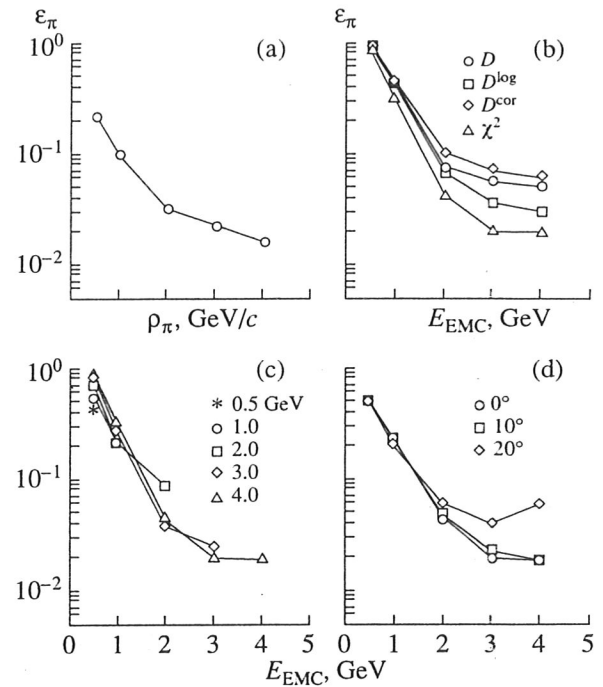


Fig. 3. The dependence of the π^+ -meson detection efficiency on (a) pion momentum p_π using criterion (2); (b) shower energy E_{EMC} measured in the calorimeter using the cuts according to (6)–(9) at $p_\pi = 4 \text{ GeV}/c$; (c) shower energy-release measured in the calorimeter using the χ^2 cuts (9) for $p_\pi = 0.5, 1, 2, 3$, and $4 \text{ GeV}/c$; and (d) shower energy-release measured in the calorimeter using the χ^2 cuts (9) for $0^\circ, 10^\circ$, and 20° angles of incidence and $p_\pi = 4 \text{ GeV}/c$. In all figures, the electron-detection efficiency is 90%.

this case, the information from all of the cluster cells is used, enhancing the separation efficiency for electromagnetic and hadronic showers. The value of the χ^2 -criterion is calculated for an event:

$$\chi^2 = \sum_i \frac{(E_i^{\text{pred}} - E_i^{\text{meas}})^2}{\sigma_i^2}, \quad (9)$$

where E_i^{meas} is the measured energy release in the i th calorimeter cell, and $E_i^{\text{pred}} = E_{\text{cell}}(x_i - X_{CG}, y_i - Y_{CG})$ is the average energy deposited in the calorimeter cell as a function of the coordinates of the shower center of gravity (X_{CG}, Y_{CG}) with respect to the center of the cell (x_i and y_i are the coordinates of the center of the cell). By analogy with [9] (see also [10]), we used the errors $\sigma_i = \sigma(E_i^{\text{pred}})$ tuned for the parameterized energy release in the calorimeter cells, which roughly described the fluctuations of energy deposited by an electromagnetic shower in the calorimeter cells

$$\sigma_i^2 = CE_i^{\text{pred}} \left(1 - \frac{E_i^{\text{pred}}}{E_0} \right) + q, \quad E_0 = \sum_i E_i^{\text{meas}}. \quad (10)$$

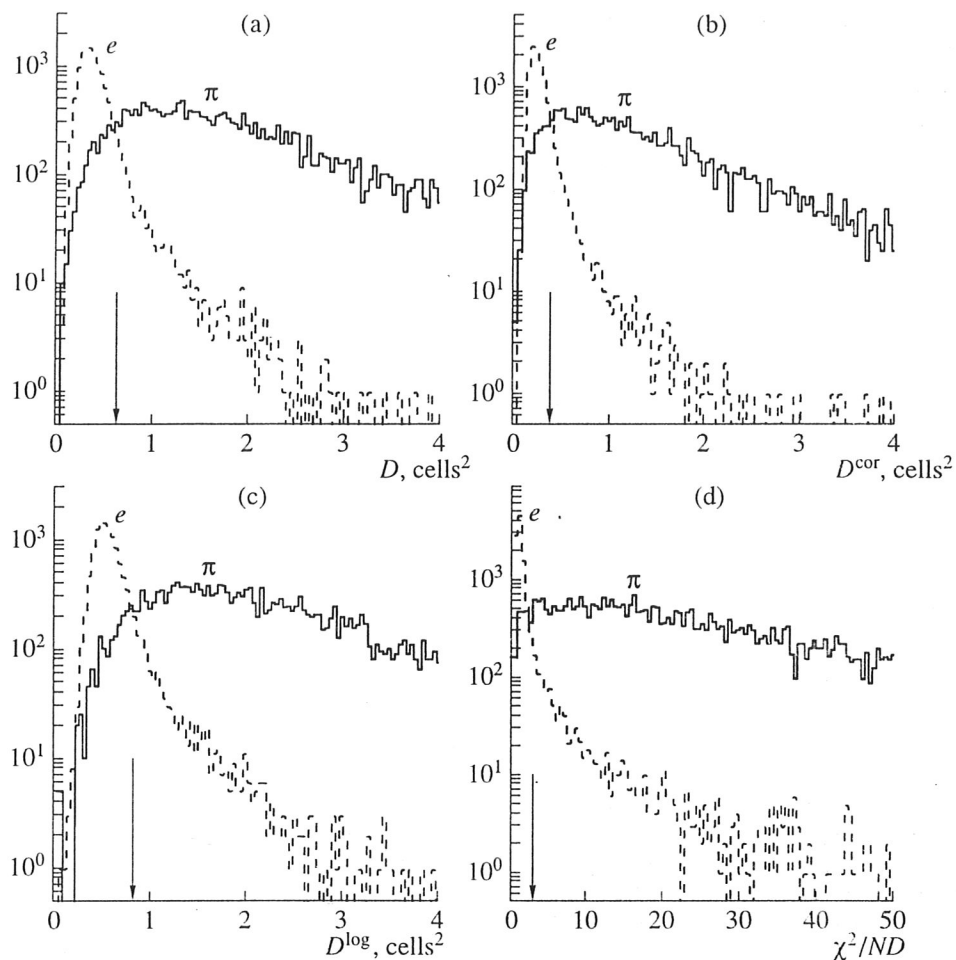


Fig. 4. The distributions of values for (a) D according to (6), (b) D^{corr} (7), (c) D^{\log} (8), and (d) χ^2 (9) for 2-GeV electrons and pions (only the events with approximately 2-GeV energy deposited in the calorimeter are taken into consideration). The cut limits, corresponding to the 90% detection efficiency for electromagnetic showers, are marked with arrows.

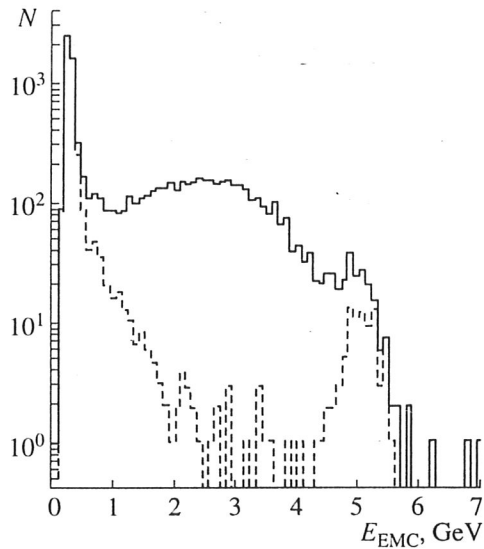


Fig. 5. The spectrum of energy deposited in the calorimeter by a π -meson beam containing $\sim 1\%$ of electrons, at 5-GeV/c beam momentum before and after applying the χ^2 cut (solid and dashed histograms, respectively).

The constant q describes the electronic noise; the constant C determines the scale of fluctuations of the energy deposited by a showering particle.

The χ^2 distribution for electromagnetic and hadronic showers with 2-GeV momentum (and energy deposited in the calorimeter of about 2 GeV), produced by charged pions, is shown in Fig. 4d. Taking into account in (9) the energies deposited in all of the calorimeter cells permits increasing the efficiency of discrimination between electromagnetic and hadronic showers by a factor of 1.5–2 in comparison with the methods based on the shower-width (D , D^{cor} , and D^{\log}) measurements (see Fig. 3b). Figure 3c presents the detection efficiency for π -mesons with momenta of 0.5, 1, 2, 3, and 4 GeV/c, on applying a cut at χ^2 , corresponding to 90% electron-detection efficiency.

The efficiency of using the shower-profile measurements for the e/π rejection is illustrated in Fig. 5. By means of the χ^2 criterion, we succeeded in extracting the electron peak (the electron impurity in the beam

was $\sim 1\%$) in the spectrum of energy deposited by a pion beam with 5-GeV energy.

The profile description of the electromagnetic showers generated by the particles that are incident at some angle with the normal to the calorimeter surface [9] permits using the method (9) for particles with non-orthogonal incidence on the calorimeter. The description is based on the parameterization of the energy deposited in the calorimeter cell on the distance between its center and the center of gravity of the shower as a function of energy and the angle of incidence. By way of example, Fig. 3d presents the detection efficiencies for 4-GeV π -mesons (ϵ_π) versus energy deposited in the calorimeter at 0° , 10° , and 20° angles of incidence. The detection efficiency for electrons (photons) remains at a level of 90%. Separation of electromagnetic and hadronic showers is virtually unchanged up to an angle of 10° . At larger angles, the longitudinal shower fluctuations in projection on the frontal calorimeter plane become significant. As a result, the shower-profiles broaden, and the $e(\gamma)/\pi$ -separation deteriorates.

METHOD BASED ON MEASURING THE SHOWER-AXIS POSITION

If there is a possibility of measuring the position of incidence on the calorimeter using a track detector, the pion rejection may be additionally improved by applying a cut to the difference between the particle coordinates measured in the calorimeter and determined with track systems.

To link the recorded tracks with the clusters of the calorimeter cells that have come into action, it is necessary to estimate the feasibility of determining the position of the hadron incidence on the calorimeter by energies deposited in the calorimeter towers (cells).

For noninteracting hadrons that are normally incident to the calorimeter surface, in most cases, positions of incidence can be measured with an accuracy up to the calorimeter cell. For the nonorthogonal incidence on the calorimeter, the particle tracks pass through several calorimeter towers, and the energy deposited in each of them is proportional to the length of the particle track traversing this tower. In this case, the position of incidence can be determined to a good degree of accuracy using the center of gravity of the cluster as a position estimate:

$$X_{CG} = \sum x_i E_i / \sum E_i, \quad (11)$$

where x_i and E_i are the position of the center and the signal value for the i th cluster cell. However, the position calculated using (11) is shifted relative to the true position of incidence by the value

$$\Delta x_{mip} = \frac{l}{2} \tan(\theta), \quad (12)$$

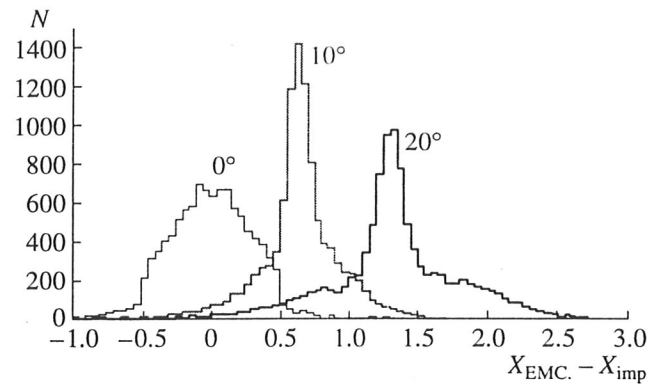


Fig. 6. The distribution of the difference between the position of impact X_{imp} and the position X_{EMC} , measured in the calorimeter, for 0° , 10° , and 20° angles of incidence at $p_\pi = 2 \text{ GeV}/c$.

where l is the calorimeter-module length and θ is the angle of incidence with respect to the normal to the calorimeter surface.

For pions that have caused a hadronic cascade in the calorimeter, the position estimation (11) is also shifted. Moreover, there is a logarithmic dependence on the particle energy E

$$\Delta x_h = (a + b \ln(E)) \tan(\theta), \quad (13)$$

where a and b are the constants, and their measured values are 16 and 3.2 cm, respectively. For pions with 2-GeV energy, $\Delta x_{mip} \approx \Delta x_h$.

By analogy with electromagnetic showers [11], the angular dependence of the accuracy of position determination according to (11) for the interacted hadrons can be represented in the form

$$\sigma_x \approx c \oplus (d \sin(\theta)). \quad (14)$$

The parameters c and d are virtually constant up to a π -meson energy of 2 GeV. Their measured values are ~ 1.7 and ~ 8.3 cm, respectively.

The position resolution improves slightly with increasing hadron energy; e.g., for 5-GeV pions, the parameters c and d are ~ 1.4 and ~ 7.2 cm, respectively.

We should note here that rigorously considering the shift of position estimation and the accuracy of position measurement according to (11) for hadrons producing a cascade in the calorimeter is dependent on the energy the hadrons deposit in the calorimeter, as well as on their energy and angle of incidence on the calorimeter. However, variations of systematic shift and position resolution for different values of energy deposited in the calorimeter do not exceed in magnitude the value of σ_x determined from (14).

Figure 6 shows the distribution of the difference between the position of the π -meson entrance measured with the wire chamber and the center of gravity of the shower calculated according to (11) for 2-GeV pion tra-

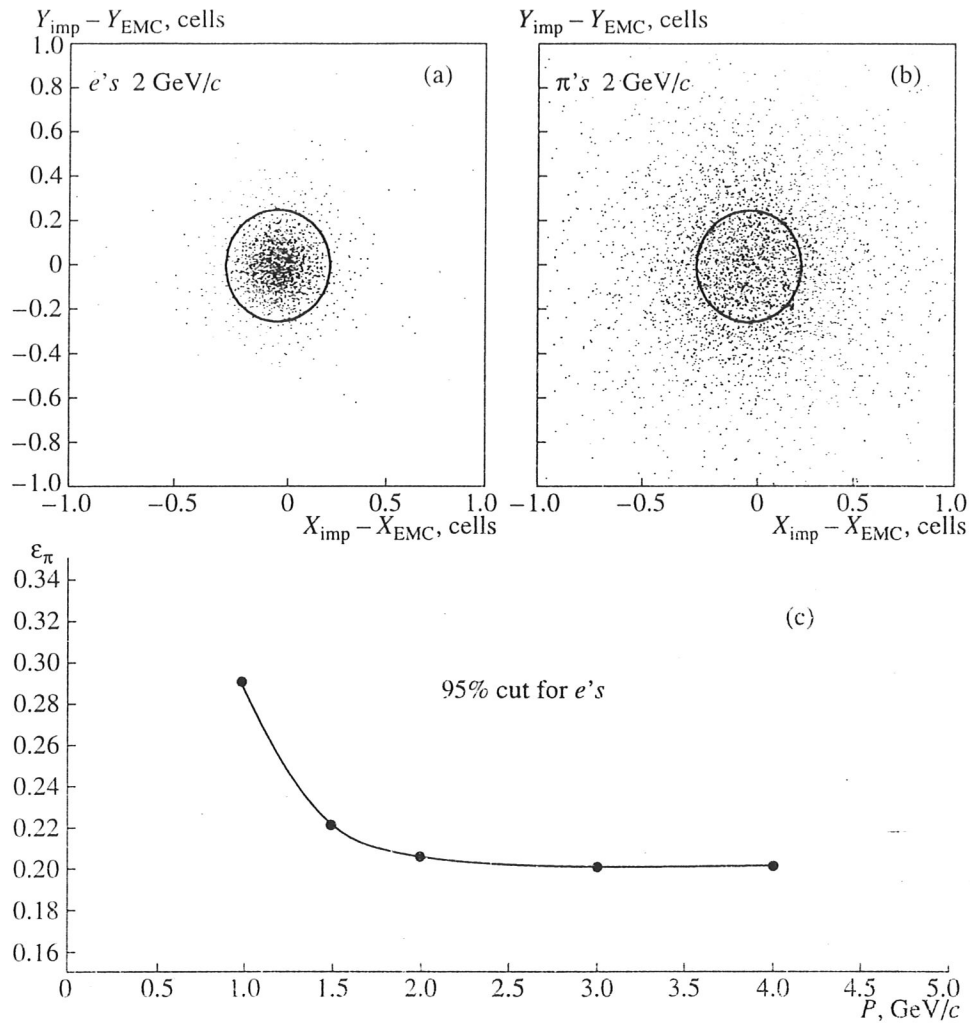


Fig. 7. The distribution of deviations of the positions measured in the calorimeter ($X_{\text{EMC}}, Y_{\text{EMC}}$) from the impact point ($X_{\text{imp}}, Y_{\text{imp}}$): (a) for electrons, (b) for interacted π^+ -mesons with $2 \text{ GeV}/c$ momentum at orthogonal incidence on the calorimeter (the cut limit corresponding to the 95% electron-detection efficiency is shown with a circle), and (c) the π -meson detection efficiency in the method based on the measurement of the shower-axis coordinates (see Figs. 7a, 7b), as a function of p_π .

versing the calorimeter at angles of incidence of 0° , 10° , and 20° . At nonorthogonal incidence of hadrons, the peak corresponding to the non-interacting hadron appears in the distribution (the hadron track passes through several calorimeter towers, and the position resolution abruptly improves).

Setting a cut at a difference between the positions of incidence, measured in the calorimeter ($X_{\text{EMC}}, Y_{\text{EMC}}$) and determined with the track systems ($X_{\text{imp}}, Y_{\text{imp}}$, see Figs. 7a, 7b), it is possible to suppress up to 80% of showering pions, keeping the electron-detection efficiency at a level of 95% (Fig. 7c). However, being applied in combination with, e.g., the χ^2 -criterion, this method permits additional rejection of only 30–50% of the hadrons, which is the outcome of the correlation for these methods.

CONCLUSION

Various methods of discrimination between electrons (photons) and hadrons were analyzed in the 0.5 – 4 -GeV range of measured energy releases in the electromagnetic calorimeter of the PHENIX setup. We studied the methods based on comparing the energy deposited in the calorimeter and the particle momentum, measuring the shower width, calculating χ^2 , and measuring the difference between the calculated and measured positions of particle incidence.

The χ^2 -criterion, which takes into account the a priori knowledge of the shower profiles, improves the $e(\gamma)/\pi$ separation by a factor of 1.5–2 in comparison with the methods based on the measurements of the shower widths only. The discrimination efficiency between the electromagnetic and hadronic showers using the χ^2 -criterion is virtually constant up to 10° angles

of incidence. At large angles, the $e(\gamma)/\pi$ rejection deteriorates, which is related to fluctuations of the cascade-curve projection onto the calorimeter plane. As the Monte Carlo simulation has shown (see also [4]), with increasing pion energy, the $e(\gamma)/\pi$ separation falls from approximately $E_{\text{EMC}} = 4 \text{ GeV}$, which is the outcome of increasing the contribution of the electromagnetic component to the value of energy (E_{EMC}) deposited by a hadronic shower in the calorimeter.

Combining these methods, one can obtain the ratio of the pion to electron detection efficiencies $\epsilon_\pi/\epsilon_e \sim (2-4) \times 10^{-4}$ for particles with $4\text{-GeV}/c$ momenta, keeping the electron-detection efficiency at $\sim 80\%$.

ACKNOWLEDGMENTS

We are grateful to all of the members of the PHENIX staff, who took part in the sessions of 1995–1996 at the AGS accelerator, for their help in the data acquisition and analysis.

REFERENCES

1. *PHENIX Conceptual Design Report*, 1993.
2. David, G., Kistenev, E., Patwa, A., et al., *IEEE Trans. Nucl. Sci.*, 1996, vol. 43, no. 3, p. 1491.
3. Review of Particle Properties, *Phys. Rev. D: Part. Fields*, 1992, vol. 45, no. 11.
4. Appuhn, R.-D., Arndt, C., Barschke, E., et al., *Nucl. Instrum. Methods Phys. Res., Sect. A*, 1996, vol. 382, pp. 395–412.
5. Davydov, V.A., Inyakin, A.V., Kachanov, V.A., et al., *Nucl. Instrum. Methods Phys. Res., Sect. A*, 1997, vol. 145, p. 267.
6. Berger, F., Bock, D., Clewing, G., et al., *Nucl. Instrum. Methods Phys. Res., Sect. A*, 1992, vol. 321, p. 152.
7. Gomez, J., Velasco, J., and Maestro, E., *Nucl. Instrum. Methods Phys. Res., Sect. A*, 1987, vol. 262, p. 284.
8. Awes, T.C., Obenshain, F.E., Plasil, F., et al., *Nucl. Instrum. Methods*, 1992, vol. 311, p. 130.
9. Bazilevsky, A. et al., *PHENIX Note*, 1998 (in press).
10. Lednev, A., *Preprint of Inst. of High-Energy Phys.*, Protvino, 1993, no. 93-153.
11. Bazilevskii, A., Durum, A., Kistenev, E., et al., *Preprint of Inst. of High-Energy Phys.*, Protvino, 1998, no. 98-17.

